

Broadband enhancement of infrared absorption in microbolometers using Ag nanocrystals

Jerome K. Hyun¹, Chi Won Ahn¹, Woo Choong Kim, Tae Hyun Kim, Moon Seop Hyun, Won-Oh Lee, Hee Yeoun Kim¹, and Jae Hong Park¹

Citation: *Appl. Phys. Lett.* **107**, 253102 (2015); doi: 10.1063/1.4937900

View online: <http://dx.doi.org/10.1063/1.4937900>

View Table of Contents: <http://aip.scitation.org/toc/apl/107/25>

Published by the [American Institute of Physics](#)

Broadband enhancement of infrared absorption in microbolometers using Ag nanocrystals

Jerome K. Hyun,^{1,a)} Chi Won Ahn,^{2,a)} Woo Choong Kim,² Tae Hyun Kim,² Moon Seop Hyun,² Won-Oh Lee,³ Hee Yeoun Kim,^{2,b)} and Jae Hong Park^{2,b)}

¹Department of Chemistry and Nano Science, Ewha Womans University, Seoul 120-750, South Korea

²National Nano-Fab Center, Daejeon 305-701, South Korea

³S-Package Solution Co., Ltd., Daegu 702-701, South Korea

(Received 22 September 2015; accepted 1 December 2015; published online 21 December 2015)

High performance microbolometers are widely sought for thermal imaging applications. In order to increase the performance limits of microbolometers, the responsivity of the device to broadband infrared (IR) radiation needs to be improved. In this work, we report a simple, quick, and cost-effective approach to modestly enhance the broadband IR response of the device by evaporating Ag nanocrystals onto the light entrance surface of the device. When irradiated with IR light, strong fields are built up within the gaps between adjacent Ag nanocrystals. These fields resistively generate heat in the nanocrystals and underlying substrate, which is transduced into an electrical signal via a resistive sensing element in the device. Through this method, we are able to enhance the IR absorption over a broadband spectrum and improve the responsivity of the device by $\sim 11\%$.

© 2015 AIP Publishing LLC. [<http://dx.doi.org/10.1063/1.4937900>]

Rationally designed infrared (IR) absorption for thermal detection or emission is a rapidly developing field with practical implications for thermally active devices. In many cases, the designed structures have taken on the form of metamaterials where geometrically tailored electromagnetic resonances in the IR give rise to spectrally selective absorption bands.^{1,2} Such characteristics are particularly useful for detecting spectrally selective sources because the background noise can be significantly reduced, leading to enhanced performance of the device.³ Metamaterials offer exciting possibilities in such regard, but from a practical standpoint, they suffer from high production costs due to multiple fabrication steps and prove challenging to implement broadband detection and imaging of IR radiation.

Traditionally, microbolometers have been a popular choice for detecting IR radiation over a broadband spectrum.⁴ In general, the device consists of an electrical sensor coupled to a thermal mass. IR radiation is absorbed by the thermal mass giving rise to a change in temperature, which is read into an electrical signal via change in resistivity of the electrical sensor. Current research on microbolometers centers on improving the responsivity of the device, where one straightforward approach is to absorb more IR radiation. In this work, we present a simple and cost-effective solution for enhancing the IR responsivity of standard microbolometer arrays over a broadband spectrum by increasing IR absorption and heat generation through a high density of randomly distributed Ag nanocrystals on their top surfaces.

Random Ag or Au nanocrystals have been thoroughly exploited in various light detection applications, especially in the visible regime where plasmonic resonances reside. Enhancements in the photoluminescence,⁵ photocurrent,⁶ electroluminescence,⁷ and Raman signals⁸ due to randomly

distributed plasmonic nanocrystals have been reported for various nanostructures and devices. While such schemes are similar in nature to our proposed system, a fundamental difference in the origin of the enhancement underscores the distinct spectral responses. Whereas the enhancements in the visible range occur due to narrowband plasmonic resonances originating from collective oscillations in the bulk of the nanocrystals, the resonances in the IR originate due to the strong expulsion of field from the interior of the nanocrystal as the metal increasingly behaves like a perfect conductor. This gives rise to strong broadband electromagnetic field enhancements in the gaps between adjacent nanocrystals.⁹ Resistively driven by the enhanced fields, heat is generated from the Ag nanocrystals and the supporting film, contributing to the thermal sensitivity of the device. One of the strongest advantages of this approach is the ease and versatility with which the nanocrystals can be prepared. Unlike the sophisticated designs and lithographic processes required to create narrowband resonances with metamaterials, the random distribution and orientation of nanocrystals can be effortlessly formed through a one-step deposition process. Through this approach, we increased the IR absorption in an array of microbolometers by an average of 11% over a broadband IR spectrum spanning from 5 to 15 μm , while increasing the responsivity by 11% at 10 μm .

Our experiments employed amorphous Si (a-Si)-based micro-bolometers that were fabricated using multiple MEMS processes consisting of completely dry procedures and CMOS-compatible materials. The fabrication involved the simultaneous fashioning of an anchor and floating membrane that consisted of a SiN_x substrate, a-Si resistor, and Ti absorption layer. Each unit was suspended 2.5 μm above an Al reflective plate for the purpose of assisting the absorption at a quarter of the target wavelength, 10 μm , by Fabry-Perot interference. The device consisted of sequential layers of SiN_x , Ti, a-Si, and SiN_x , with thicknesses of 100, 15, 100,

^{a)}J. K. Hyun and C. W. Ahn contributed equally to this work.

^{b)}Authors to whom correspondence should be addressed. Electronic addresses: hyeounkim@nnfc.re.kr and jhpark@nnfc.re.kr

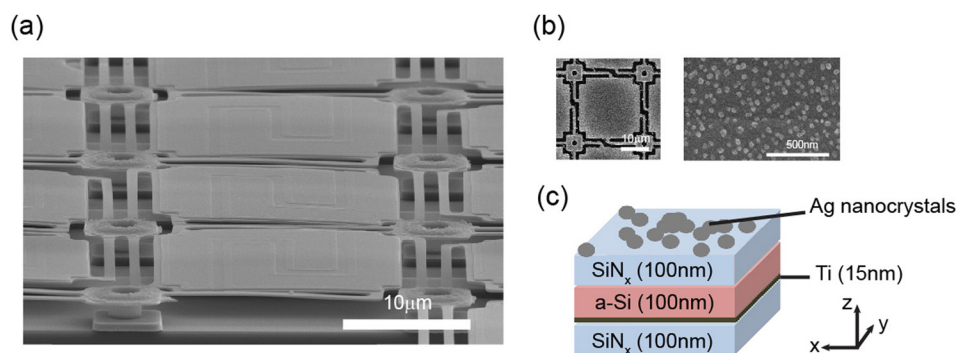


FIG. 1. (a) SEM image of fabricated microbolometers arrays. (b) Low (left panel) and high (right panel) magnification SEM images of the top surface of a single microbolometer unit supporting Ag nanocrystals. (c) Schematic of a microbolometer unit.

and 100 nm, respectively (Figure 1(c)). The Ti layer serves as a thermal mass, converting IR radiation to heat, while simultaneously forming the basis for two lateral electrodes separated by an S-shaped gap, as shown in Figure 1(a). The a-Si layer serves as the electrical sensor, having a high temperature coefficient of resistance. SiN_x films were prepared using a PECVD process.

We introduced Ag nanocrystals onto post-fabricated microbolometer arrays. Ag nanocrystals were evaporated directly on top of the SiN_x surface at a rate of 1 nm/min with a targeted thickness close to 10 nm. Figure 1(b) shows SEM images of the surface of a single microbolometer unit supporting Ag nanocrystals at low (left panel) and high (right panel) magnification. Being under the percolation threshold,^{10,11} nucleated nanocrystals remained in an island form. The characteristic size of the nanocrystals was near 50 nm.

In order to evaluate the response of Ag nanocrystals on microbolometers when irradiated with IR light, we compared the absorption from microbolometers before and after the deposition of Ag nanocrystals, as shown in Figure 2. IR radiation was focused to a 500 μm-sized spot using a reflective objective, covering approximately 20 × 20 devices. In the wavelength range of interest from 5 to 15 μm, microbolometer arrays with Ag nanocrystals showed an absorption enhancement from 4% to 17% relative to the bare microbolometer arrays. We note that the absence of Fabry-Perot enhancement in our measurements is likely due to the incoherent light source, inhomogeneities among individual microbolometers within the illumination spot, and scattering off the edges and posts of the microbolometer units.

We used 3D Finite difference time domain (FDTD) simulations to elucidate the absorption enhancing role of the Ag nanocrystals when coupled to IR radiation in a single microbolometer unit. In order to focus on the interaction between IR radiation and the Ag nanocrystals, we used a plane wave source and excluded the reflective bottom layer and posts in our treatment while restricting the lateral size of the system to 1 × 1 μm². In order to expedite the calculations and to effectively remove numerical instabilities at the lateral boundaries, we applied periodic boundary conditions to the lateral boundaries and maintained perfectly matched layers for the top and bottom boundaries. This simplification approximates the random nature of the system, but is sufficient in providing the critical insight required at the nanoscale level without the large computational demands involved with wider areas. Furthermore, the period is much less than the wavelengths of interest such that grating-induced diffractive effects are

absent. In order to simulate an unpolarized source, we averaged the responses from two sources exhibiting orthogonal polarizations. The nanocrystals were modeled as randomly distributed spherical particles exhibiting a size distribution centered about 50 nm, emulating the topography viewed by SEM. The dielectric functions for Ag, a-Si, and Ti were found from Palik.¹² For simplification purposes, SiN_x was modeled with a lossless dielectric constant of 2.

The upper panel of Figure 3(a) displays the total absorption within the device for the case with and without the Ag nanocrystals. One can observe that with the Ag nanocrystals the device dissipates up to 25% more power than without the nanocrystals in the wavelength range from 5 to 15 μm, which agrees with the enhanced absorption, as shown in Figure 2. However, we note that the absolute value of the measured absorption for the bare reference from Figure 2 is on average greater than the calculated absorption. This discrepancy can be accounted by our exclusion of loss components in both the a-Si and SiN_x films in our model. In fact, SiN_x films should exhibit some loss in the IR due to asymmetric stretching vibration of the Si-N bonds and can vary in extent depending on fabrication conditions (i.e., temperature).^{13,14} We also note that impurities may introduce a small finite imaginary component to the dielectric function, which generates absorption.

In order to assess the distribution of power within the thermal mass, we also calculated absorption in the Ti layer as shown in the lower panel of Figure 3(a). For the case of

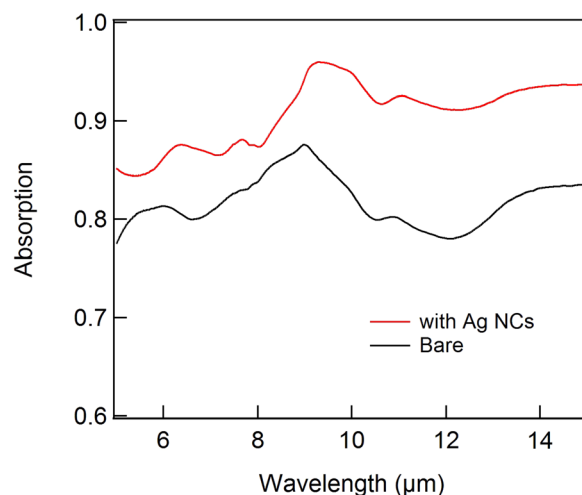


FIG. 2. Absorption spectrum from microbolometer arrays before (black curve) and after (red curve) deposition of Ag nanocrystals.

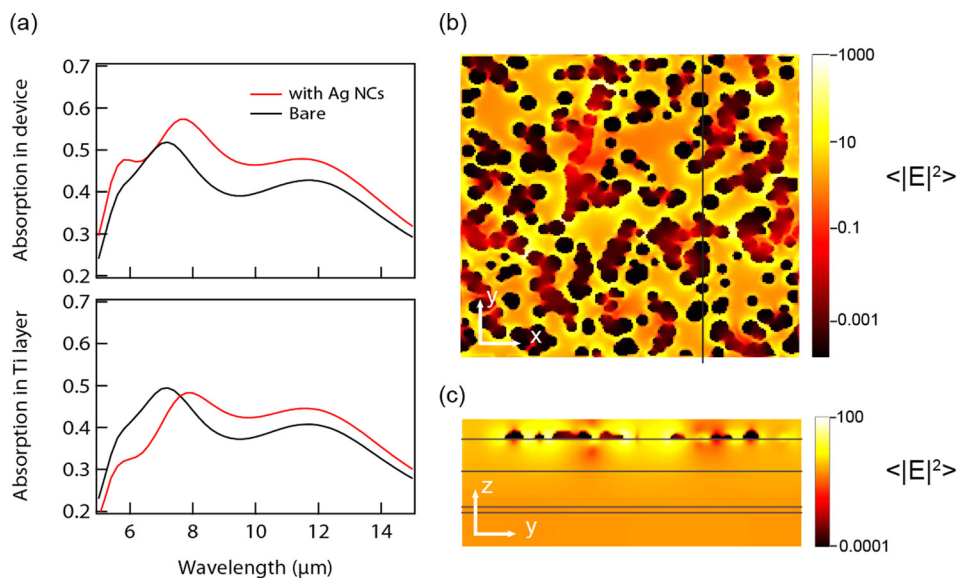


FIG. 3. Calculated responses of unpolarized IR radiation in a microbolometer device using 3D FDTD simulations. (a) Absorption spectrum in device (top panel) and the Ti layer (bottom panel) with (red curve) and without (black curve) Ag nanocrystals. (b) Planar field intensities occurring 5 nm above the surface of the SiN_x film at a wavelength of $10\ \mu\text{m}$. Size of the map is $1 \times 1\ \mu\text{m}^2$. (c) Field intensities occurring in a yz -cross-section at $x = 210\text{ nm}$, indicated by the black line in (b) at a wavelength of $10\ \mu\text{m}$. The map spans $1\ \mu\text{m}$ in the y -direction and 375 nm in the z -direction.

the bare microbolometer, the absorption spectrum stays almost identical to that of the entire device, as Ti is the main absorbing unit and the other layers were modeled without loss components in the IR. With the introduction of Ag nanocrystals, absorption in the Ti layer is either enhanced or suppressed depending on the wavelength, as shown in Figure 3(a). This suggests two functions of the Ag nanocrystals. The function responsible for the suppression in absorption arises from the Ag nanocrystals shadowing or scattering away the radiation from the Ti layer. The second function responsible for the enhanced absorption is the scattering of radiation into the Ti layer.

Solid Ag nanoparticles do not exhibit a plasmonic resonance in the mid IR. In fact, in the mid IR, the Ag increasingly behaves as a perfect conductor, expelling fields from its interior. A previous report described this effect in regular arrays of Ag nanoshells, invoking the “lightning-rod” effect to describe the strong field expulsion from an array of Au shells. Such phenomenon gives rise to enhanced fields in the gaps between the shells, whose resonance spans across a broadband range in the IR.⁹ The broadband nature of the response was identified as collective dipolar resonances and associated radiative damping in constrained spatial volumes smaller than the wavelength of light. Electric field distributions monitored at a wavelength of $10\ \mu\text{m}$, shown in Figures 3(b) and 3(c), similarly demonstrate this behavior. Figure 3(b) describes the field intensity, shown on a log scale, 5 nm above the surface of the top SiN_x layer. Localized bright hot spots are visible near the surface of the nanoparticles and particularly enhanced in the gaps between nanoparticles, with intensity values between 10 and 1000. Intensity is also visible within the bodies of the nanoparticles despite the strong expulsion of IR field. Nevertheless, as the imaginary part of the permittivity increases for larger wavelengths, we can deduce that the small field penetration into the nanoparticles may induce finite absorption, responsible for the increase in the absorption, as shown in Figure 3(a). The absorption represents power dissipation through high surface currents in the nanoparticles, leading to the generation of heat as has been previously reported by other groups.^{15,16}

Another source of heat generation due to the strong field intensity can be found from the SiN_x layer. A y - z cross-section of the field intensity at $x = 210\text{ nm}$, indicated by the black line, is displayed in Figure 2(c). Here, bright intensity is observed in between adjacent nanoparticles and is shown to penetrate into the underlying SiN_x substrate. Although our model does not take into account absorption of the SiN_x layer due to the absence of imaginary components in the permittivity, we can deduce that in reality the film must generate heat at positions subjected to high field intensities. In essence, the Ag nanocrystals and the SiN_x substrate act as an additional heat source driven by the IR light, raising the temperature and resulting in a larger change in resistivity of the a-Si detection layer.

The effect of the enhanced IR absorption on device performance was demonstrated by monitoring the average current of 10 individual devices under bias, before and after the deposition of Ag nanocrystals. The devices were measured in a probe station under vacuum levels of approximately $5 \times 10^{-2}\text{ Torr}$. A 0.7 V operating bias voltage was determined from breakdown tests of the device driven from 0.2 to 1 V. The IR source power was maintained at 2.25 W, while a shutter was used to turn the source on and off. After measuring the response from a bare set of devices at $10\ \mu\text{m}$, Ag crystals were deposited on the same devices and measured under the same conditions to demonstrate the effect of the Ag crystals. The inset of Figure 4 shows that with the Ag nanocrystals, IR radiation induces a steady-state current, measured from 0.02 to 0.1 s, which is close to $0.99\ \mu\text{A}$, whereas without the Ag nanocrystals the device reaches a steady-state current of $0.98\ \mu\text{A}$. When no IR radiation impinges on the devices, the steady-state current is equivalently $0.9\ \mu\text{A}$ for the case with and without the Ag nanocrystals. Herein, the variable of interest is the change in current induced by turning on the IR light. Figure 4 describes this change in current, converted into responsivity, where the nanocrystals are shown to improve the steady-state responsivity from 34.9 to $38.9\ \text{nA/W}$, corresponding to an $11.5 \pm 0.4\%$ enhancement. We note that because single pixels were measured instead of a pixel array and because the signal was not amplified, the absolute responsivity was found in the nA/W range.

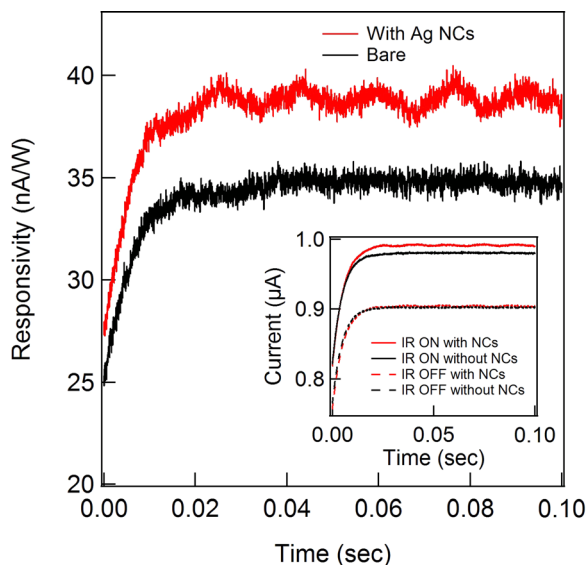


FIG. 4. Responsivity as a function of time from devices before (black curve) and after (red curve) deposition of Ag nanocrystals. Inset: Current as a function of time with IR radiation on (solid curves) and off (dotted curves) for devices before and after deposition of Ag nanocrystals.

In short, we have described a simple but effective approach to enhance the responsivity of microbolometers using randomly distributed Ag nanocrystals. Without using any lithographical processes normally required for designed nanostructures, the Ag nanocrystals can be formed directly on top of post-fabricated microbolometers through a one-step deposition process, resulting in modest absorption and responsivity enhancements. The enhancement in absorption is broadband due to the nature of the IR dipolar resonances driven in unison within gaps between adjacent Ag nanocrystals. Device performance at $10\ \mu\text{m}$ indeed demonstrates that the Ag nanocrystals improve the responsivity of the device by 11%. These results suggest cheap and quick pathways for enhancing the performance limits of existing microbolometers.

This work was supported by the Daedeok Technology Business Program (ACC-2013-DGI-00557) GRDC(2015K1A4A3047100), Basic Science Research program (2012R1A1A2007707), and the Global Frontier program (2014M3A6B3063706) funded by the Ministry of Science, ICT and Future Planning through the National Research Foundation of Korea (NRF). The authors also acknowledge support from the Open Innovation Lab Project from the National Nanofab Center (NNFC), the Ewha Womans University Research Grant of 2015, and the TJ Park Science Fellowship through the POSCO TJ Park Foundation.

- ¹F. B. P. Niesler, J. K. Gansel, S. Fischbach, and M. Wegener, *Appl. Phys. Lett.* **100**, 203508 (2012).
- ²H. Tao, N. I. Landy, C. M. Bingham, X. Zhang, R. D. Averitt, and W. J. Padilla, *Opt. Express* **16**, 7181 (2008).
- ³J. J. Talghader, A. S. Gawarikar, and R. P. Shea, *Light-Sci. Appl.* **1**, e24 (2012).
- ⁴F. Niklaus, C. Vieider, and H. Jakobsen, *Proc. SPIE* **6836**, 68360D (2008).
- ⁵T. Sakashita, Y. Miyauchi, K. Matsuda, and Y. Kanemitsu, *Appl. Phys. Lett.* **97**, 063110 (2010).
- ⁶J. K. Hyun and L. J. Lauhon, *Nano Lett.* **11**, 2731 (2011).
- ⁷J. B. Khurgin, G. Sun, and R. A. Soref, *Appl. Phys. Lett.* **93**, 021120 (2008).
- ⁸B. Sharma, R. R. Frontiera, A. I. Henry, E. Ringe, and R. P. Van Duyne, *Mater. Today* **15**, 16 (2012).
- ⁹F. Le, D. W. Brandl, Y. A. Urzhumov, H. Wang, J. Kundu, N. J. Halas, J. Aizpurua, and P. Nordlander, *ACS Nano* **2**, 707 (2008).
- ¹⁰P. Pavaskar, I. K. Hsu, J. Theiss, W. H. Hung, and S. B. Cronin, *J. Appl. Phys.* **113**, 034302 (2013).
- ¹¹A. L. Efros and B. I. Shklovskii, *Phys. Status Solidi B-Basic Solid State Phys.* **76**, 475 (1976).
- ¹²E. D. Palik, *Handbook of Optical Constants of Solids* (Academic, Orlando, 1985).
- ¹³M. Molinari, H. Rinnert, and M. Vergnat, *Appl. Phys. Lett.* **77**, 3499 (2000).
- ¹⁴D. Della Sala, C. Coluzza, G. Fortunato, and F. Evangelisti, *J. Non-Cryst. Solids* **77-78**, 933 (1985).
- ¹⁵A. O. Govorov and H. H. Richardson, *Nano Today* **2**, 30 (2007).
- ¹⁶G. Baffou, R. Quidant, and F. J. G. de Abajo, *ACS Nano* **4**, 709 (2010).